Vol. 738: 75–87, 2024
https://doi.org/10.3354/meps14595

MARINE ECOLOGY PROGRESS SERIES
Mar Ecol Prog Ser

Published June 20

Dealing with biases introduced by lipids in stable carbon and nitrogen isotope analyses: a solution based on 28 marine invertebrate, fish, and mammal species

Jean-François Ouellet, Jory Cabrol, Ève Rioux, Xavier Bordeleau, Véronique Lesage*

Marine Mammals Biology and Conservation, Maurice-Lamontagne Institute, Fisheries and Oceans Canada, Mont-Joli, Québec G5H3Z4, Canada

ABSTRACT: Stable carbon ($\delta^{13}C$) and nitrogen ($\delta^{15}N$) isotope ratios are widely used in marine food web and habitat use studies. However, lipids are naturally depleted in ^{13}C relative to proteins and are variable in content, biasing $\delta^{13}C$ of bulk samples, with consequences for the accuracy of conclusions. This issue can be resolved either by extracting lipids from samples prior to analysis, a resource-intensive process that can also alter $\delta^{15}N$, or by estimating lipid-free $\delta^{13}C$ using one of several equations that differ in degree of sophistication and generalization across taxa. Here, $\delta^{13}C$ and $\delta^{15}N$ were measured in bulk and lipid-extracted muscle samples from over 2000 specimens of 28 species of marine invertebrates, fishes, and mammals. Our objectives were to compare the effect of lipid extraction on $\delta^{13}C$ and $\delta^{15}N$ across taxa and evaluate the performance of 5 normalization models, overall and using subsets of species, to propose a model to revert lipid-extracted $\delta^{15}N$ back to their bulk values and to identify the best approach for dealing with lipid-related biases. Lipid extraction caused an uneven enrichment in $\delta^{13}C$ and $\delta^{15}N$ across species. Model taxonomic specificity increased estimation accuracy for both isotopes. While models from Logan et al. (2008; J Anim Ecol 77:838–846) and McConnaughey & McRoy (1979; Mar Biol 53:257–262) were the best at predicting lipid-free $\delta^{13}C$, a linear model reliably estimated $\delta^{15}N$ values of lipid-free samples using $\delta^{15}N$ values of bulk samples. This study presents a method for reliably estimating $\delta^{13}C$ and $\delta^{15}N$ values of muscle tissue without resorting to duplicate analyses. This represents a major step toward the harmonization of data sets generated using bulk and lipid-extracted samples.

KEY WORDS: Marine species · Carbon and nitrogen isotopes · Lipid · Lipid extraction · Lipid normalization · Mixture model · Stable isotopes

1. INTRODUCTION

Some chemical elements are present in animal tissues in the form of stable isotopes that differ in specific mass. The proportion of heavy to light isotopes of a specific element varies according to multiple environmental and biological drivers. For example, the lighter carbon and nitrogen isotopes (^{12}C and ^{14}N, respectively) are generally metabolized and excreted preferentially over their heavier counterparts (e.g. ^{13}C and ^{15}N; Peterson & Fry 1987, Hobson et al. 1996). As a result, heavier isotopes tend to accumulate more and more predictably in animal tissues than lighter isotopes, making stable isotopes useful tracers of carbon sources and trophic position, and thereby habitat use and movement patterns across isoscapes (Hobson 1999, Post 2002, Perrin et al. 2014).

Despite their broad utilization in trophic ecology studies, an important confounding factor of stable isotope analyses has been variability in the lipid content of samples, given that lipids are naturally depleted in ^{13}C relative to proteins or other biochemical

*Corresponding author: veronique.lesage@dfo-mpo.gc.ca

Publisher: Inter-Research · www.int-res.com

compounds (DeNiro & Epstein 1977). The lipid content of animal tissues can vary over time and space with a myriad of factors, including health and body condition, reproductive status, or season. The presence and variability of lipids within and among species may lead to misinterpretation of changes in diet or habitat use. The importance of this issue was underestimated during the early developments of the method, and samples were considered as pure proteins. However, consensus quickly built about the need to assess potential effects of lipids on $\delta^{13}C$ values and, if significant, to account for this bias (Hobson et al. 1996, Post et al. 2007, Choy et al. 2016). Lipid extraction prior to isotope analysis has become a popular approach for dealing with lipid-related biases. This procedure is based on the assumption that an absence of nitrogenous components in chemical solvents would prevent alteration of $\delta^{15}N$ values. However, this assumption was refuted by empirical assessments, with multiple studies across a variety of species reporting significant and uneven effects of lipid extraction on $\delta^{15}N$ values, although generally toward a ^{15}N enrichment of tissues (Choy et al. 2016, Clark et al. 2019, Lerner & Hunt 2022, but see Cloyed et al. 2020). An alternative to lipid extraction has been to analyze carbon and nitrogen isotopes using separate aliquots (Logan et al. 2008, Lesage et al. 2010). The consequent doubling of analytical costs and time increased the interest in lipid normalization models for $\delta^{13}C$ values, leading to numerous proposed approaches with various levels of sophistication and generalization (McConnaughey & McRoy 1979, Fry et al. 2003, Logan et al. 2008, Lesage et al. 2010, Clark et al. 2019, Fischer-Rush et al. 2021). Empirical comparison of models showed various levels of performance across taxonomic groups and tissues (Logan et al. 2008), emphasizing the importance of model validation and specificity. Variability in the ways that investigators handle the issue of ^{13}C depletion associated with lipids may hinder comparisons among studies. As a result, caution and validation are needed when selecting a model for a particular taxon or tissue, including coefficient values. However, thus far, little guidance exists for investigators in making that choice. In addition, models for reverting lipid-extracted $\delta^{15}N$ values back to their bulk un-extracted values, and thus making older data sets (in which lipid-extraction was the norm) suitable for long-term monitoring of environmental or trophic change, are few (Logan et al. 2008, Lesage et al. 2010, Groß et al. 2021, Lerner & Hunt 2022). A variety of tissues are amenable to stable isotope analysis, integrating signatures over periods varying from hours to years (Vander Zanden et al. 2015). Muscle is a popular tissue sampled in studies of food web structure as it integrates diet over periods of weeks to months (Vander Zanden et al. 2015), is constituted for the most part of pure protein, and is relatively easily available for many food web components (e.g. Lesage et al. 2001, Hobson et al. 2002).

Here, we take advantage of a large data set of over 2000 specimens from 28 marine species including invertebrates, bony and cartilaginous fishes, and marine mammals, for which both lipid-extracted and bulk $\delta^{13}C$ and $\delta^{15}N$ values have been determined for muscle tissue to improve our understanding of these questions. Specifically, we (1) compared the effect of chemically extracting lipids on $\delta^{13}C$ and $\delta^{15}N$ across taxa; (2) examined the relative performance of 5 popular mathematical normalization models for estimating lipid-free $\delta^{13}C$, both overall and for subsets of resembling species; (3) proposed a model to restore old data sets in which lipid extraction was applied systematically to all samples, and thus revert lipid-free $\delta^{15}N$ values to their bulk values; and (4) identified the most suitable approach for dealing with lipid effects on isotopic values, including the best models and parameters to use for a given data set or particular taxa. This study represents a major step toward the harmonization of data sets collected under different approaches for long-term studies.

2. MATERIALS AND METHODS

2.1. Sample collection

Our sample consisted of 2222 muscle samples from 28 species of marine invertebrates, bony and cartilaginous fishes, and mammals collected opportunistically between 2010 and 2021 (see Table 1 & Table S1 in the Supplement at www.int-res.com/articles/suppl/m738p075_supp.pdf) in the Estuary and Gulf of St. Lawrence, Canada. Most of the fish and invertebrate specimens were obtained through an annual trawling mission (Bourdages et al. 2019). Additional samples were obtained from various scientific missions and sampling programs, commercial fisheries using fish traps, or opportunistic netting. Beluga *Delphinapterus leucas* samples were obtained post-mortem from well-preserved to moderately decomposed beach-cast carcasses (freshness code 2 or 3; Geraci & Lounsbury 1993), whereas grey seal *Halichoerus grypus* samples were obtained from scientific or commercial harvests conducted in the Magdalen Islands (Gulf of St. Lawrence). Given that our sampling pro-

gram was largely opportunistic, the number of specimens sampled per year varied greatly across species, with some years lacking sampling altogether (see Tables 1 & S1). All samples were frozen upon collection in air-tight plastic bags and stored at −20°C.

Muscle samples were excised dorso-laterally from fishes (~1.5 g), grey seals (~1.5 g), and beluga (~500 cm^3). The whole dorsal muscle without the carapace was taken from euphausiids and northern shrimps *Pandalus borealis*, and the mantle was taken from northern shortfin squids *Illex illecebrosus*. Samples were minced, freeze-dried for 48 h, and ground to a fine powder with a mortar and pestle (Wig-L-Bug, Crescent Dental). Samples were then divided into 2 aliquots: one aliquot received no further treatment prior to isotope analysis (bulk); the second aliquot was lipid-extracted.

Lipids were extracted using a 2:1 (v:v) chloroform and methanol mixture following the procedure described by Folch et al. (1957) and outlined in Lesage et al. (2010). Briefly, ~0.2 g of powdered muscle was mixed with 10 ml of the chloroform and methanol mixture, sonicated for 15 min, and stored overnight at 4°C with gentle shaking. The sample was then centrifuged for 10 min at 1500 rpm (251 × *g*) and the supernatant discarded. The lipid extraction process was repeated twice, with the exception that the mixture was put on an agitator plate for 1 h instead of overnight. After extraction, samples were desiccated by evaporation and dried overnight at 60°C.

Subsamples of 0.350–0.500 mg of homogenized muscle tissue were precisely weighted and encapsulated in tin capsules. $\delta^{13}C$ and $\delta^{15}N$ values, along with the percentage of carbon (%C) and nitrogen (%N) content, were measured in bulk and lipid-free aliquots of each sample using a continuous-flow stable-isotope mass spectrometer coupled to a Carlo Erba elemental analyzer (CHNS-O EA1108). Isotope ratios are expressed in delta (δ) notation in parts per thousand (‰) difference from a standard (Vienna Pee Dee Belemnite limestone and atmospheric N for ^{13}C and ^{15}N, respectively) and calculated as $\delta X = [(R_{sample} / R_{standard}) - 1] \times 1000$, where X is ^{13}C or ^{15}N and R is the corresponding $^{13}C/^{12}C$ or $^{15}N/^{14}N$ value. The C:N ratio was calculated as the ratio of %C to %N. The accuracy of isotopic analyses was assessed using commercially certified material (acetanilide or nicotinamide), and precision was assessed by replicating measurements every 10 samples in the series. The analytical error was ±0.1‰ for $\delta^{13}C$ and ±0.3 for $\delta^{15}N$ based on laboratory standards; the repeatability for replicates was 0.2‰ for $\delta^{13}C$, 0.2‰ for $\delta^{15}N$, 0.94% for %C, and 0.30% for %N (n = 466).

2.2. Statistical analyses and normalization models

Paired *t*-tests with a Bonferroni correction were used to examine, for each species, the effect of lipid extraction on $\delta^{13}C$ and $\delta^{15}N$. The difference between lipid-free and bulk aliquots was expressed as $\Delta\delta^{13}C$ ($\delta^{13}C_{lipid\text{-}free} - \delta^{13}C_{bulk}$) and $\Delta\delta^{15}N$ ($\delta^{15}N_{lipid\text{-}free} - \delta^{15}N_{bulk}$). The degree of discrimination against ^{13}C is known to be related to the $C{:}N_{bulk}$ ratio in a log-linear relationship (Logan et al. 2008, Lesage et al. 2010, Fischer-Rush et al. 2021, Lerner & Hunt 2022), and this relationship was tested here.

The potential for lipid normalization of $\delta^{13}C$ values using $\delta^{13}C_{bulk}$ was estimated with 5 models that have been commonly used in the literature over the past decade. These models varied both in structure (linear and non-linear models) and in the set of constant parameters they included. The MM model (McConnaughey & McRoy 1979) is a non-linear model developed using the whole body of various marine vertebrates and invertebrates:

$$\delta^{13}C_{lipid\text{-}free} = \delta^{13}C_{bulk} + D \times \left[I + \frac{3.90}{\left(1 + \frac{287}{L}\right)} \right] \quad (1)$$

where

$$L = \frac{93}{1 + \left(0.246 \times C{:}N_{bulk} - 0.775\right)^{-1}}$$

and where I is a constant (equal to −0.207), L is the lipid content, and D is the isotopic difference between pure protein and pure lipids (assumed to be 6‰; McConnaughey & McRoy 1979). The Fry model (Fry 2002), customarily referred to as the mass-balance approach, was developed using muscle tissue from freshwater fish species:

$$\delta^{13}C_{lipid\text{-}free} = \delta^{13}C_{bulk} + D - \left(\frac{D \times C{:}N_{lipid\text{-}extracted}}{C{:}N_{bulk}} \right) \quad (2)$$

where D is again the isotopic difference between pure protein and pure lipid. The Post model (Post et al. 2007), is a linear model developed using aquatic species (muscle or whole organisms):

$$\delta^{13}C_{lipid\text{-}free} = \delta^{13}C_{bulk} + \beta_0 + \beta_1 \times C{:}N_{bulk} \quad (3)$$

where the intercept (β_0) equals −3.32 and the slope (β_1) is 0.99. The Logan model (Logan et al. 2008) is a log-linear relationship developed using freshwater and marine species and multiple tissues:

$$\delta^{13}C_{lipid\text{-}free} = \delta^{13}C_{bulk} + \beta_0 + \beta_1 \times \ln\left(C{:}N_{bulk}\right) \quad (4)$$

where $\beta_0 = -4.763$ and $\beta_1 = 4.401$ for fish muscle tissue. Finally, the Lesage model (Lesage et al. 2010) is a linear model developed for cetacean skin. It is the

sole model tested that did not take C:N ratios into account:

$$\delta^{13}C_{lipid\text{-}free} = \beta_0 + \beta_1 \times \delta^{13}C_{bulk} \quad (5)$$

where $\beta_0 = -4.334$ and $\beta_1 = -0.331$.

In contrast with carbon stable isotopes for which we seek to estimate $\delta^{13}C_{lipid\text{-}free}$ values, for nitrogen isotopes, it is generally $\delta^{15}N_{bulk}$ that we seek to estimate and restore from lipid-extraction biases. Given that $\delta^{15}N_{bulk}$ is expected to be linearly related to $\delta^{15}N_{lipid\text{-}free}$ (Logan et al. 2008, Lesage et al. 2010, Groß et al. 2021, Lerner & Hunt 2022), this relationship was tested here (see Section 3.1) to accurately retro-estimate $\delta^{15}N_{bulk}$ from $\delta^{15}N_{lipid\text{-}free}$.

$$\delta^{15}N_{bulk} = \beta_0 + \beta_1 \times \delta^{15}N_{lipid\text{-}free} \quad (6)$$

2.3. Model performance

Model performance was assessed by linearly regressing predicted values against observed values ($\delta^{13}C_{lipid\text{-}free}$ or $\delta^{15}N_{bulk}$) and by examining the mean absolute error (MAE) and accuracy in predictions, calculated as the relative proportion of predicted values falling within the mean measurement error (0.2‰ for both $\delta^{13}C$ and $\delta^{15}N$) of observed values. The slopes of these relationships were also compared with a target value of 1.00 (perfect relationship). The coefficient of determination (r^2) and Akaike information criterion (AIC) were calculated for within-group comparison (see Section 2.4) of carbon normalization models.

2.4. Model specificity

The precision of estimates and model fit are expected to improve with sample size but also with data specificity (i.e. specific tissue and species; Logan et al. 2008, Lesage et al. 2010, Cloyed et al. 2020). In an attempt to fulfill these conflicting conditions, a trade-off was reached by dividing the sample into clusters of resembling species. Here, species resemblance was defined as a similarity in the species response to lipid extraction rather than phylogenetic kinship (i.e. based on similarity in C:N ratios or isotopic values; details provided below). Normalization models were therefore run according to 4 scenarios that differed in sample size and data specificity. The comparison of model performance across scenarios allowed us to check if doing so actually improved model fit. The 'global approach' scenario aimed at maximizing sample size: all specimens were combined and the models were run on a single cluster of 2222 specimens. In the 'cluster-based' scenario, the models were run on smaller clusters of species that were defined using mixture models (R package 'flexMix'; Leisch 2004, Grün & Leisch 2007, 2008). Mixture models are a convenient tool for distributing items in an optimized number of clusters based on similarities in their relationship with an independent variable (Hamel et al. 2017). Here, the clusterization was based on the relationship of $\delta^{13}C_{bulk}$ against $C{:}N_{bulk}$ for $\delta^{13}C$ and that of $\delta^{15}N_{bulk}$ against $\delta^{15}N_{lipid\text{-}free}$ for $\delta^{15}N$. The optimal number of clusters (k) was determined using the 'stepFlexMix' function (R package 'flexMix') and Bayesian information criterion (BIC) after repeated trials with candidate values of k ranging from 1 to 28, the maximum number of species. The uneven number of years of sampling across species (Table S1) excluded the possibility of accounting for temporal autocorrelation in the clusterization equations. However, a visual examination of the residuals plotted against year showed that the temporal autocorrelation was probably negligible (Fig. S1). In the 'species-specific' scenario, each species was individually considered as a cluster, maximizing model specificity. Finally, in the 'original coefficients' scenario, the models were run on clusters of species like in the cluster-based scenario but using the originally published coefficient values (presented with each equation in Section 2.2), thereby reducing model specificity to our particular data set. In the global approach, cluster-based, and species-specific scenarios, least-squares estimates of coefficients were obtained for each combination of model and cluster with function 'nls2' (R package 'nls2'; Grothendieck 2022) for predicting $\delta^{13}C_{lipid\text{-}free}$ and with the function 'refit' (R package 'flexMix') for predicting $\delta^{15}N_{bulk}$. The performance of the various models and scenarios for grouping species or estimating coefficients was evaluated by comparing results with a model where all specimens were included in a single linear regression (predicted vs. observed value).

The sensitivity of our clustering approach and model predictions was examined for the global, cluster-based, and species-specific approach by proceeding with the species clustering using 70% randomly selected observations for each species within our original data set and repeating this procedure 3 times. Performances of the predictive models for $\delta^{13}C$ and $\delta^{15}N$ were assessed by using the clusters identified with the full data set, from which 70% of observations were randomly selected to build the model and

the remaining 30% of observations were used for model testing. All lipid-normalization models were tested in the case of carbon isotopes. Change in model performance was based on percent change in performance indicators (slope, MAE, r^2).

All statistical analyses were performed using R software version 4.2.2 (R Core Team 2022). Homogeneity of variance and normality assumptions were tested for each statistical analysis where relevant.

3. RESULTS

3.1. Effect of lipid extraction on isotopes and C:N ratios

Lipid extraction caused a significant enrichment in both $\delta^{13}C$ and $\delta^{15}N$ values for all species (paired *t*-tests; $t > 3.5$, df > 9, $p < 0.002$ for each species) except for $\delta^{13}C$ in grey seal *Halichoerus grypus* ($t = -0.9$, df = 203, $p = 0.38$), northern krill *Meganyctiphanes norvegica* ($t = 2.7$, df = 12, $p = 0.02$), shorthorn sculpin *Myoxocephalus scorpius* ($t = 3.3$, df = 8, $p = 0.01$), thorny skate *Amblyraja radiata* ($t = 2.2$, df = 12, $p = 0.05$), and witch flounder *Glyptocephalus cynoglossus* ($t = 3.9$, df = 8, $p = 0.005$) and for $\delta^{15}N$ in beluga *Delphinapterus leucas* ($t = 1.0$, df = 61, $p = 0.31$), shorthorn sculpin ($t = 3.4$, df = 8, $p = 0.01$), and witch flounder ($t = 3.2$, df = 8, $p = 0.01$). Mean effect size varied across species from 0.0 to 2.0‰ for $\delta^{13}C$ and from 0.1 to 1.1‰ for $\delta^{15}N$ (Table 1, Fig. 1a,b) and exceeded measurement errors in all cases with the exception of grey seal and thorny skate for $\delta^{13}C$ (Fig. 1a), and beluga and thorny skate for $\delta^{15}N$ (Fig. 1b). Species showing the largest $\delta^{13}C$ enrichment following lipid extraction were predictably those with the highest $C:N_{bulk}$ ratios, as shown by the non-linear relationship between these variables (Fig. 1c). Such a relationship with $C:N_{bulk}$ ratios was non-existent for $\delta^{15}N$ ($F_{1,26} = 1.5$, $p = 0.23$; data not shown). However, our data showed, as expected based on published studies (e.g. Logan et al. 2008, Lesage et al. 2010, Groß et al. 2021, Lerner & Hunt 2022), a linear relationship between $\delta^{15}N_{bulk}$ and $\delta^{15}N_{lipid\text{-}free}$ (Fig. 1d).

3.2. Identifying groups of resembling species

Based on the 'stepFlexMix' function and lowest BIC, the optimal number of clusters of resembling species within our data set was 8 for $\delta^{13}C$ and for $\delta^{15}N$ (Table 2). Posterior probabilities (i.e. the probability for a species to be adequately assigned to a cluster, indicative of the robustness of the clusterization output) were high for both isotopes, with means and medians of 0.95 and 1.00 for the classification based on carbon (C-classification) and 0.93 and 1.00 for the classification based on nitrogen (N-classification). The relationships used to discriminate the clusters (ratios of $\delta^{13}C_{bulk}$ vs. $C:N_{bulk}$ and $\delta^{15}N_{bulk}$ vs. $\delta^{15}N_{lipid\text{-}free}$) were generally negative for the C-classification with the exception of cluster B, which was composed of northern shrimp *Pandalus borealis* and white hake *Urophycis tenuis*, and was positive for the N-classification (Fig. 2). Clusters differed in species composition between the C- and N-classifications, and in both cases showed little apparent taxonomic correlation within clusters: species belonging to the same family were seldom clustered together (Table 2, Fig. 3).

Proceeding with the cluster analysis using a reduced set (70%) of the data still produced robust clusters (posterior probability of accurate assignment still close to 1), and a structure with 7–8 clusters identified for carbon and 5–6 clusters for nitrogen, depending on clustering iteration (3 were performed). A few species switched groups, suggesting some sensitivity to sample composition.

The comparison of model performances across all scenarios for the 2 isotopes showed that regardless of the lipid-normalization model selected, model fit was invariably the best in the species-specific scenario (Table 3). Model performances were consistently the poorest in the global approach scenario, with a 0.1‰ average increase in MAE and an average loss of relative accuracy of 10% compared to the species-specific scenario. The cluster-based scenario was intermediate between the global approach and species-specific scenarios but showed a smaller deviance from the species-specific than global approach scenario (Table 3), with an average increase in the MAE of 0.03‰ and average decrease in relative accuracy of 3%.

Model fit was consistently best when $\delta^{13}C$ was normalized using model coefficient values optimized with our data set, as in the cluster-based scenario, instead of when using the original published values, as in the original coefficients scenario. The gain in model performance from optimized coefficient values was the greatest in MM and Lesage models and the smallest in Fry and Logan models. Model coefficient values optimized for each combination of cluster and model are shown in Table 4. Coefficient *D*, involved in the MM and Fry models, stands as a discrimination factor between pure proteins and pure lipids and was

Table 1. Sample size (n), size range of specimens (mass in g for krill and total length in cm for all other species), mean (SD) C:N ratios, and stable isotope ratios (in ‰) for carbon and nitrogen ($\delta^{13}C$, $\delta^{15}N$) of muscle samples from species under study, including differences between lipid-extracted (LE) and bulk values ($\Delta\delta^{13}C$, $\Delta\delta^{15}N$). NA: not available

Family	Species	n	Size range	$\delta^{13}C_{bulk}$	$\delta^{13}C_{LE}$	$\Delta\delta^{13}C$	$\delta^{15}N_{bulk}$	$\delta^{15}N_{LE}$	$\Delta\delta^{15}N$	C:N_{bulk}	C:N_{LE}
Invertebrates											
Euphausiidae	Arctic krill *Thysanoessa* spp.	16	0.3–0.5	−18.8 (1.2)	−18.2 (0.9)	0.6 (0.6)	9.1 (0.3)	9.7 (0.2)	0.5 (0.3)	3.8 (0.3)	3.1 (0.2)
	Northern krill *Meganyctiphanes norvegica*	13	0.3–0.5	−19.4 (0.4)	−19.0 (0.5)	0.4 (0.6)	10.3 (0.4)	10.8 (0.5)	0.5 (0.2)	3.5 (0.1)	3.0 (0.1)
Ommastrephidae	Northern shortfin squid *Illex illecebrosus*	30	13–20.8	−19.9 (0.3)	−19.0 (0.4)	0.9 (0.3)	12.5 (0.3)	13.1 (0.3)	0.6 (0.4)	3.4 (0.1)	3.1 (0.0)
Pandalidae	Northern shrimp *Pandalus borealis*	251	2–17	−18.7 (0.8)	−18.2 (0.7)	0.4 (0.3)	12.0 (0.5)	12.7 (0.6)	0.7 (0.4)	3.2 (0.1)	3.0 (0.1)
Fishes											
Ammodytidae	Sand lance *Ammodytes* sp.	49	6.5–15.4	−20.2 (0.9)	−19.6 (0.9)	0.6 (0.3)	10.9 (0.9)	11.7 (0.8)	0.8 (0.4)	3.3 (0.1)	3.1 (0.1)
Anguillidae	American eel *Anguilla rostrata*	16	58–74.2	−24.0 (3.5)	−22.1 (3.4)	1.9 (0.6)	13.0 (1.1)	13.5 (1.1)	0.5 (0.4)	5.6 (0.9)	3.1 (0.1)
Clupeidae	Atlantic herring *Clupea harengus*	194	7.8–32.9	−21.5 (0.9)	−19.8 (0.6)	1.7 (0.8)	12.4 (0.6)	13.4 (0.7)	1.0 (0.5)	4.7 (1.1)	3.1 (0.1)
Cottidae	Longhorn sculpin *Myoxocephalus octodecemspinosus*	10	16.3–27	−18.5 (0.6)	−18.0 (0.4)	0.5 (0.3)	12.5 (0.5)	13.5 (0.6)	0.9 (0.1)	2.8 (0.0)	2.8 (0.0)
	Shorthorn sculpin *Myoxocephalus scorpius*	9	16.3–32.1	−18.0 (0.8)	−17.6 (0.7)	0.4 (0.4)	14.3 (0.7)	15.0 (0.7)	0.6 (0.6)	3.1 (0.2)	2.9 (0.3)
Gadidae	Arctic cod *Boreogadus saida*	124	7.5–20	−20.5 (0.8)	−19.8 (0.6)	0.7 (0.4)	12.6 (0.7)	13.3 (0.6)	0.7 (0.4)	3.3 (0.1)	3.1 (0.1)
	Atlantic cod *Gadus morhua*	192	11.2–46	−19.5 (0.8)	−19.1 (0.9)	0.4 (0.4)	14.0 (0.9)	14.6 (0.9)	0.6 (0.4)	3.1 (0.2)	3.0 (0.2)
	Atlantic tomcod *Microgadus tomcod*	26	15.4–31.1	−18.2 (0.9)	−17.9 (0.9)	0.2 (0.2)	15.5 (0.5)	16.2 (0.5)	0.8 (0.3)	3.3 (0.1)	3.0 (0.1)
Liparidae	Atlantic seasnail *Liparis atlanticus*	11	8.2–15.5	−19.3 (0.3)	−18.9 (0.2)	0.5 (0.2)	12.9 (0.5)	13.6 (0.5)	0.7 (0.3)	3.2 (0.1)	3.1 (0.0)
Merlucciidae	Silver hake *Merluccius bilinearis*	18	23.7–42.5	−20.0 (0.4)	−19.3 (0.3)	0.6 (0.4)	13.5 (0.5)	14.1 (0.4)	0.7 (0.2)	3.5 (0.3)	3.1 (0.0)
Moronidae	Striped bass *Morone saxatilis*	53	18.7–55.5	−18.2 (1.3)	−17.8 (1.3)	0.4 (0.4)	15.2 (1.0)	15.6 (0.9)	0.4 (0.3)	3.3 (0.2)	3.0 (0.1)
Osmeridae	Capelin *Mallotus villosus*	190	9.5–17.3	−20.6 (0.6)	−19.6 (0.6)	1.0 (0.5)	12.3 (0.5)	13.2 (0.5)	0.9 (0.4)	3.6 (0.5)	3.1 (0.1)
	Rainbow smelt *Osmerus mordax*	24	14.7–22.5	−19.5 (1.3)	−19.3 (1.4)	0.2 (0.2)	14.7 (0.6)	15.3 (0.6)	0.6 (0.3)	3.3 (0.1)	3.1 (0.1)
Phycidae	White hake *Urophycis tenuis*	43	13.4–29.7	−18.8 (0.7)	−18.4 (0.7)	0.3 (0.3)	13.4 (1.1)	14.2 (1.1)	0.7 (0.2)	3.1 (0.1)	3.0 (0.1)
Pleuronectidae	American plaice *Hippoglossoides platessoides*	195	14.6–44	−19.2 (0.8)	−18.8 (0.8)	0.4 (0.3)	13.7 (0.6)	14.3 (0.6)	0.6 (0.5)	3.2 (0.1)	3.0 (0.1)
	Greenland halibut *Reinhardtius hippoglossoides*	187	15.1–35.6	−21.1 (0.7)	−19.1 (0.6)	2.0 (0.7)	13.2 (0.7)	14.3 (0.7)	1.1 (0.5)	4.6 (1.0)	3.1 (0.1)
	Winter flounder *Pseudopleuronectes americanus*	37	6.8–34	−19.2 (0.8)	−18.5 (0.7)	0.7 (0.7)	13.5 (1.6)	14.5 (1.2)	1.0 (0.8)	3.3 (0.4)	3.0 (0.1)
	Witch flounder *Glyptocephalus cynoglossus*	9	21.6–35.5	−18.2 (0.5)	−17.9 (0.4)	0.3 (0.2)	13.9 (0.5)	14.3 (0.6)	0.4 (0.4)	3.0 (0.0)	2.8 (0.0)
Rajidae	Thorny skate *Amblyraja radiata*	13	NA	−18.2 (0.4)	−18.0 (0.3)	0.2 (0.3)	11.9 (0.6)	12.1 (0.6)	0.2 (0.1)	2.4 (0.1)	2.5 (0.0)
Scombridae	Atlantic mackerel *Scomber scombrus*	53	6.2–16.5	−20.8 (1.0)	−20.3 (0.8)	0.5 (0.5)	10.4 (0.7)	11.0 (0.7)	0.6 (0.4)	3.3 (0.2)	3.0 (0.1)
Scorpaenidae	Redfish *Sebastes* sp.	162	14.2–35.9	−19.9 (0.6)	−19.5 (0.5)	0.4 (0.4)	12.8 (1.0)	13.5 (0.9)	0.7 (0.4)	3.3 (0.3)	3.1 (0.1)
Zoarcidae	Eelpout *Lycodes* sp.	31	12.9–36.5	−18.5 (0.4)	−18.3 (0.3)	0.2 (0.4)	13.4 (0.4)	13.9 (0.5)	0.6 (0.3)	3.3 (0.1)	3.1 (0.0)
Mammals											
Monodontidae	Beluga *Delphinapterus leucas*	62	175–485	−17.9 (0.5)	−17.5 (0.4)	0.4 (0.6)	15.5 (1.2)	15.6 (1.2)	0.1 (0.5)	3.5 (0.5)	3.1 (0.2)
Phocidae	Grey seal *Halichoerus grypus*	204	NA	−18.8 (0.5)	−18.9 (0.5)	0.0 (0.4)	15.3 (0.6)	15.5 (0.6)	0.2 (0.3)	3.3 (0.1)	3.3 (0.1)

Table 2. Species composition of clusters in the carbon (C) and nitrogen (N) classifications. Clusterization was performed using the 'stepFlexMix' function (R package 'flexMix'; Leisch 2004, Grün & Leisch 2007, 2008)

Cluster	Species				
C-classification					
A	Atlantic cod	Atlantic seasnail	Northern shortfin squid	Redfish sp.	Silver hake
B	Northern shrimp	White hake			
C	American plaice	Northern krill	Winter flounder		
D	Arctic cod	Atlantic herring	Atlantic mackerel	Sandlance	
E	Arctic krill Witch flounder	Atlantic tomcod	Beluga	Shorthorn sculpin	Striped bass
F	Eelpout sp.	Grey seal	Longhorn sculpin	Thorny skate	
G	American eel	Rainbow smelt			
H	Capelin	Greenland halibut			
N-classification					
A	American plaice	Atlantic cod	American eel	Witch flounder	Shorthorn sculpin
B	Arctic cod	Atlantic mackerel	Redfish sp.	Sandlance	Northern shortfin squid
C	Atlantic herring	Capelin	Greenland halibut		
D	Silver hake Rainbow smelt	White hake Atlantic tomcod	Northern krill Atlantic seasnail	Arctic krill	Eelpout sp.
E	Beluga				
F	Northern shrimp	Longhorn sculpin			
G	Winter flounder				
H	Grey seal	Striped bass	Thorny skate		

assigned a value of 6‰ by McConnaughey & McRoy (1979) and Fry (2002). The *D* value optimized with our data set fluctuated across clusters but was generally lower than 6‰ and was lower for the MM model than the Fry model (Table 4). Coefficient values belonging to the species-specific scenario are shown in Table S2.

The MM and Logan models consistently showed the lowest MAE and the highest relative accuracy in all scenarios except in the original-coefficients scenario. Comparison of model performances within clusters was based on 3 criteria (Table 5): first, whether the slope confidence interval includes the target value of 1; second, the rank of the models in increasing order of absolute difference between their slope and the target value of 1; and third, the rank in increasing order of MAE. This comparison showed that the best model for lipid-normalizing $\delta^{13}C$ of marine species changes according to cluster composition (Tables 5 & S3). All the models, with Lesage as the only exception, were in turn identified as the best one. But again, MM and Logan were consistently either the best or second-best models. The Lesage model showed low AIC values, but all other indicators suggested poor model performance (Tables 5 & S3).

The $\delta^{15}N$ retro-correction model generally led to a slightly superior accuracy than $\delta^{13}C$ lipid-normalization models but had MAE values well within the range of $\delta^{13}C$ lipid-normalization models in all scenarios (Table 3). In the global approach scenario, the retro-correction of $\delta^{15}N$ achieved lower r^2 and slope, but also a lower MAE than most lipid-normalization models (Table S3). Differences in cluster composition between the C- and N-classifications prevented a direct comparison of model performance indicators per cluster in the cluster-based scenario. However, the retro-correction models of $\delta^{15}N$ for the different clusters had global performance indicators that were comparable to those obtained for lipid-normalization of $\delta^{13}C$ (Table S3) and in some cases (but not all), a lower MAE and greater r^2 than the model combining all species together.

Using a reduced set of data to build our models had only small effects on model performances, with performance indicators (model slope and fit) varying by less than 3% for the global approach in both isotopes and by <10% (C) and <13% (N) for the cluster-based approach. As expected, the species-based approach, which started inherently with the smallest sample size, was the most sensitive of the approaches tested, with a change in performance indicators of <28% for C and <17% for N.

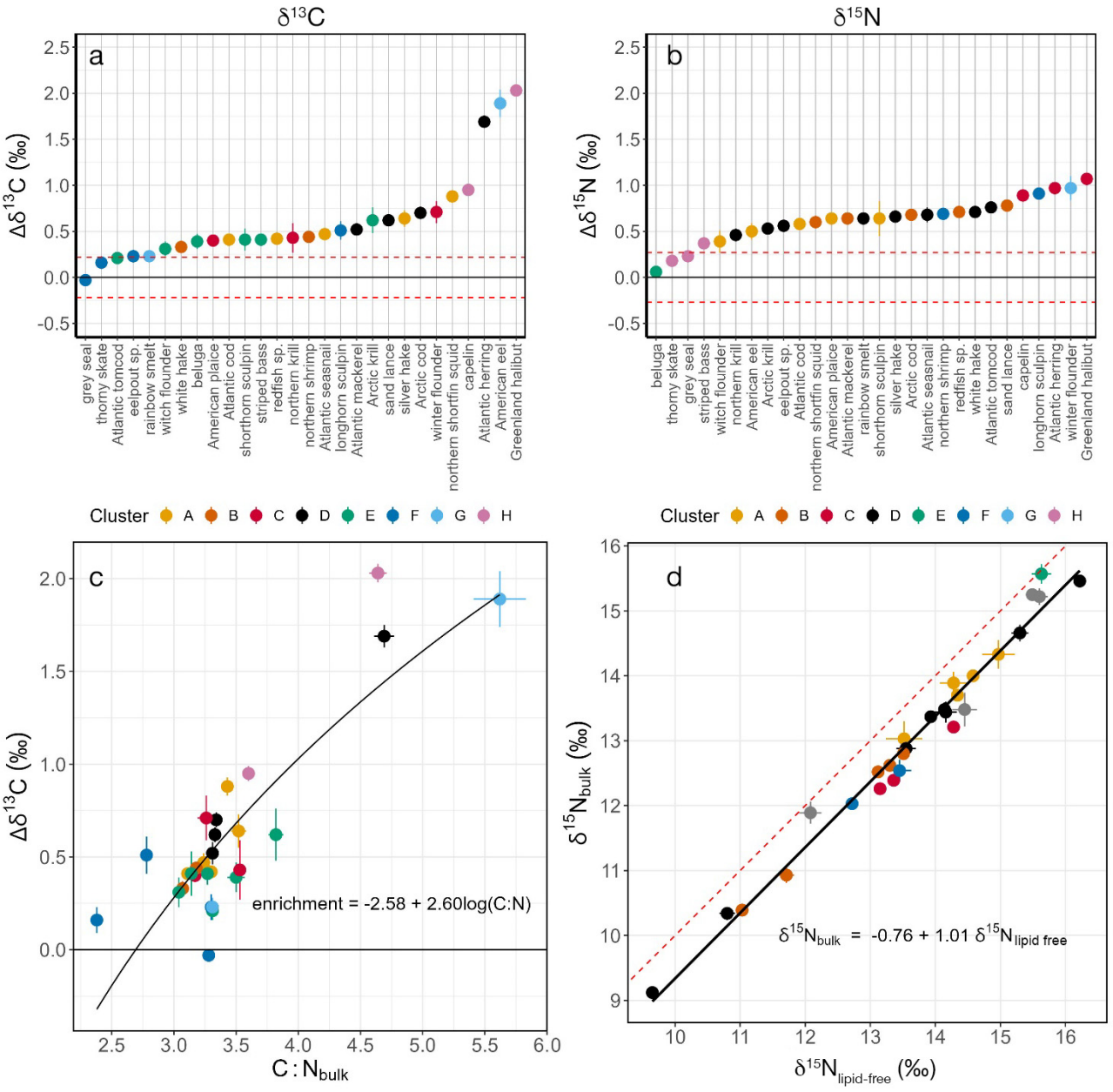

Fig. 1. Mean ± SE enrichment following lipid extraction (lipid-free − bulk) for (a) $\delta^{13}C$ and (b) $\delta^{15}N$ in 28 marine species. Species are sorted by mean value. Horizontal dashed lines: upper 95% confidence limit of intra-individual difference between replicates, above and below 0‰. (c) Relationship between mean (±SE) $\delta^{13}C$ enrichment and $C:N_{bulk}$. (d) Relationship between mean ± SE bulk and lipid-free $\delta^{15}N$ for 28 marine species; red dashed line: relationship with slope 1 and intercept 0. See Table 1 for sample sizes

4. DISCUSSION

This study advances the field of trophic ecology using isotopic tracers by providing a thorough review of the performance of existing lipid-normalization models, using a large data set (i.e. over 2000 samples) of 28 marine species. Our results indicate that while there are clear benefits in exploiting taxa- or group-specific models, some models, such as the ones developed by McConnaughey & McRoy (1979) and Logan et al. (2008), not only outperformed other models but introduced little additional error. We propose a way forward for how to best deal with lipids and lipid extraction biases in isotopic studies, including a most-needed model to restore old data sets where lipid extraction was applied systematically to all samples, to revert $\delta^{15}N_{lipid\text{-}free}$ values to their bulk values.

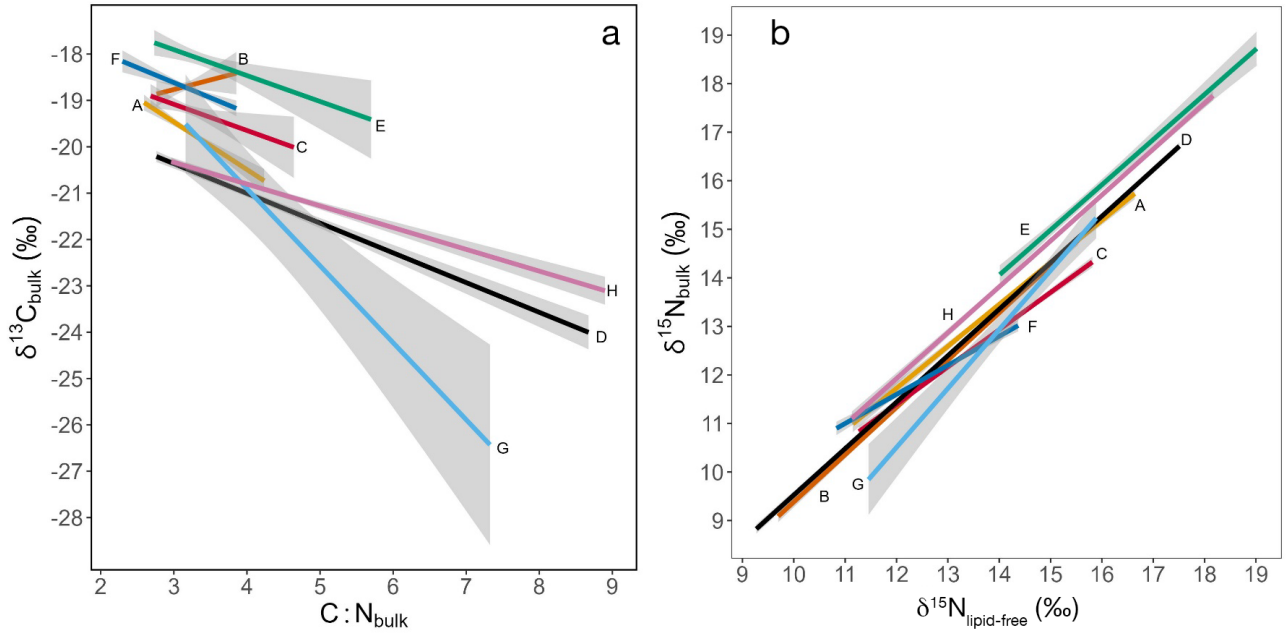

Fig. 2. Linear relationships (±95% CI) forming the basis for the clusterization procedure in the (a) C-classification ($\delta^{13}C_{bulk}$ vs. $C:N_{bulk}$) and (b) N-classification ($\delta^{15}N_{bulk}$ vs. $\delta^{15}N_{lipid\text{-}free}$), for each cluster of species. Clusterization was performed using the 'stepFlexMix' function (R package 'flexMix'; Leisch 2004, Grün & Leisch 2007, 2008). Labels indicate cluster names. Cluster composition differs between both classifications

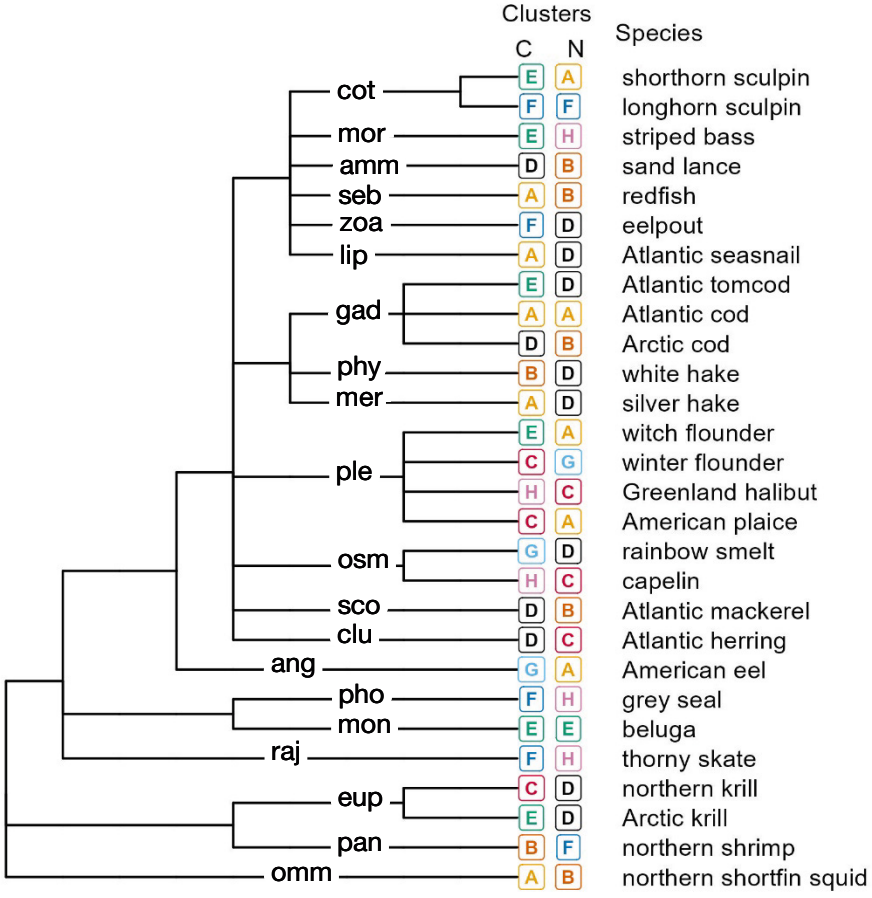

Fig. 3. Phylogeny of the 28 species in the sample and the clusters to which the species belong. C and N indicate the classifications based on carbon and nitrogen, respectively, and produced with mixture models using the 'stepFlexMix' function (R package 'flexMix'; Leisch 2004, Grün & Leisch 2007, 2008). Families are abbreviated with their first 3 letters; full names are as follows: Ammodytidae, Anguillidae, Clupeidae, Cottidae, Euphausiidae, Gadidae, Liparidae, Merlucciidae, Monodontidae, Moronidae, Ommastrephidae, Osmeridae, Pandalidae, Phocidae, Phycidae, Pleuronectidae, Rajidae, Scombridae, Sebastidae, and Zoarcidae. Label placements for families along the *x*-axis are arbitrary. Phylogenetic data were extracted from the World Register of Marine Species (WoRMS Editorial Board 2022)

Table 3. Comparison of model performance according to 4 scenarios that differ in level of data specificity (global approach, cluster-based, species-specific, original-coefficients scenarios). MAE: mean absolute error (‰); $diff_{MAE}$: difference between the MAE in a scenario and that of the best scenario within the same model (which was invariably the species-specific scenario); Acc.: relative accuracy (%; the relative proportion of predicted values falling within the mean measurement error); $diff_{acc}$: difference between the relative accuracy in a scenario and that of the best scenario within the same model. Models (Eqs. 1–5) correspond to MM (McConnaughey & McRoy 1979), Fry (Fry 2002), Post (Post et al. 2007), Logan (Logan et al. 2008), and Lesage (Lesage et al. 2010), respectively. Nitrogen (Eq. 6) refers to nitrogen lipid normalization (this study)

Model	Global approach scenario				Cluster-based scenario				Species-specific scenario		Original coefficients scenario			
	MAE	$diff_{MAE}$	Acc.	$diff_{acc}$	MAE	$diff_{MAE}$	Acc.	$diff_{acc}$	MAE	Acc.	MAE	$diff_{MAE}$	Acc.	$diff_{acc}$
MM (Eq. 1)	0.37	0.09	34.7	−10.9	0.30	0.02	41.4	−4.1	0.28	45.6	1.49	1.20	0.9	−44.7
Fry (Eq. 2)	0.35	0.03	33.6	−5.7	0.33	0.01	36.8	−2.5	0.32	39.3	0.35	0.03	34.9	−4.4
Post (Eq. 3)	0.36	0.07	35.0	−8.7	0.31	0.02	40.9	−2.9	0.29	43.7	0.61	0.32	14.2	−29.6
Logan (Eq. 4)	0.36	0.08	35.1	−9.0	0.30	0.02	41.5	−2.7	0.28	44.2	0.37	0.09	35.9	−8.3
Lesage (Eq. 5)	0.44	0.14	29.1	−13.0	0.36	0.07	35.3	−6.8	0.30	42.1	21.24	20.94	0.0	−42.1
Nitrogen (Eq. 6)	0.38	0.08	40.6	−12.1	0.31	0.01	52.1	−0.6	0.3	52.7	–	–	–	–

Table 4. Coefficient estimates of the 5 lipid-normalization models for $\delta^{13}C$ values and the model retro-correcting $\delta^{15}N_{lipid\text{-}free}$ values. Model references are the same as in Table 3. *D* represents the isotopic difference between pure protein and pure lipid, *I* is a constant, and β_0 and β_1 are the intercept and slope of the model

Scenario/cluster	$\delta^{13}C$									$\delta^{15}N$	
	MM (Eq. 1)		Fry (Eq. 2)	Post (Eq. 3)		Logan (Eq. 4)		Lesage (Eq. 5)		Eq. (6)	
	D	*I*	*D*	β_0	β_1	β_0	β_1	β_0	β_1	β_0	β_1
Global approach scenario	4.43	0.08	5.60	−2.13	0.80	−3.59	3.46	0.62	−6.80	−1.01	1.02
Cluster-based scenario											
A	2.31	0.18	5.67	−1.77	0.69	−2.15	2.24	−1.77	0.89	1.22	0.87
B	−1.08	−0.40	5.74	1.49	−0.33	1.65	−1.06	−2.45	0.85	−0.38	0.98
C	1.82	0.24	4.77	−1.56	0.63	−1.76	1.90	−3.56	0.79	2.18	0.77
D	4.51	0.09	5.38	−1.60	0.69	−3.18	3.19	−11.46	0.40	−0.05	0.96
E	2.46	0.10	3.58	−1.61	0.59	−2.23	2.15	−2.43	0.84	1.02	0.93
F	−0.17	−0.22	2.53	0.08	−0.01	0.17	−0.11	−5.71	0.69	4.56	0.59
G	4.40	0.01	4.23	−1.83	0.64	−3.35	3.02	−3.25	0.81	−4.06	1.21
H	5.02	0.1	6.3	−1.53	0.73	−3.36	3.48	−14.77	0.22	0.58	0.95

Table 5. Identification of the most performant normalization models using 3 criteria and 8 data sets (Clusters A–H in cluster-based scenario): (1) CI: whether the 95% confidence interval of the slope of a linear relationship between predicted $\delta^{13}C_{lipid\text{-}free}$ and observed $\delta^{13}C_{lipid\text{-}free}$ includes (CI = y) or not (CI = n) the target value of 1.00; (2) slope: within-cluster rank of the model based on the increasing absolute distance to target value of 1.00; (3) MAE: within-cluster rank of the model based on increasing mean absolute error. **Bold** indicates the best ranking model in each cluster. Model references are the same as in Table 3

Cluster	n	MM (Eq. 1) CI; slope; MAE	Fry (Eq. 2) CI; slope; MAE	Post (Eq. 3) CI; slope; MAE	Logan (Eq. 4) CI; slope; MAE	Lesage (Eq. 5) CI; slope; MAE
A	413	n; 1; 2	n; 2; 4	**n; 1; 1**	n; 1; 2	n; 3; 3
B	294	y; 2; 2	y; 1; 3	y; 2; 2	y; 2; 2	n; 3; 1
C	245	n; 2; 1	n; 2; 3	**n; 1; 1**	**n; 1; 1**	n; 3; 2
D	420	**y; 1; 1**	n; 3; 3	y; 2; 2	y; 2; 1	n; 4; 4
E	175	n; 2; 2	n; 1; 2	**n; 1; 1**	n; 2; 2	n; 3; 3
F	258	n; 2; 2	**n; 1; 1**	n; 2; 2	n; 2; 2	n; 3; 1
G	40	**y; 1; 1**	y; 2; 4	y; 2; 3	y; 2; 2	y; 3; 5
H	377	n; 2; 1	**n; 1; 1**	n; 3; 3	n; 2; 2	n; 4; 4

4.1. Effect of lipid extraction

Our study brought further evidence that lipid extraction results in an increase in both $\delta^{13}C$ and $\delta^{15}N$ values and that in all but a handful of species, this change exceeded the measurement error (Post et al. 2007, Logan et al. 2008, Choy et al. 2016, Clark et al. 2019, Lerner & Hunt 2022). As expected, species with the largest discrimination against ^{13}C following lipid extraction were those with the highest C:N ratios, which are often — but not always — the most lipid-rich samples (Fischer-Rush et al. 2021, but see Fagan et al. 2011, Yurkowski et al. 2015, Choy et al. 2016). The C:N ratio has been used extensively in the literature to determine whether or not lipid extraction or normalization was warranted. Generally, samples characterized by low $C:N_{bulk}$ ratios (<3.5) and low lipid content (<15%) were considered to be minimally affected by lipid extraction (Post et al. 2007, Logan et al. 2008, Skinner et al. 2016). Our study, however, documents a wide spread of $\Delta\delta^{13}C$ estimates at low C:N ratios (Fig. 1c) and argues against such an approach. With a C:N ratio of 3.5, $\Delta\delta^{13}C$ can reach up to 1‰, which may correspond to one trophic level increment in marine food webs (Peterson & Fry 1987, Stephens et al. 2022). Other authors also warned against not accounting for lipids at low C:N ratio values and recommended that the $\delta^{13}C$ depletion bias in lipids be always accounted for as a precaution (Choy et al. 2016, Rioux et al. 2019, Cloyed et al. 2020, Groß et al. 2021). $\delta^{13}C$ values of grey seal *Halichoerus grypus* were notably not affected by lipid extraction. This was also reported by Clark et al. (2019) for muscle of walruses *Odobenus rosmarus*, another pinniped species. These authors explained this result with a low lipid content in muscle tissue. Similarly, Cloyed et al. (2020) found no effect of lipid extraction on $\delta^{13}C$ in West Indian manatee *Trichechus manatus* muscle. The positive relationship observed between $\delta^{13}C_{bulk}$ and $C:N_{bulk}$ ratios in cluster B, consisting only of northern shrimp *Pandalus borealis* and white hake *Urophycis tenuis*, was atypical compared to other clusters. However, this was only a weak relationship with a high p-value (0.21) and low r^2 (0.01), and a narrow range of $C:N_{bulk}$ ratios. Although the $C:N_{bulk}$ ratio was not a good predictor for $\delta^{13}C_{bulk}$ in these particular species, the lipid-normalization model performed adequately.

4.2. Model performances

The linear relationship observed between bulk and lipid-free $\delta^{15}N$ was consistent with multiple previous studies (i.e. Logan et al. 2008, Lesage et al. 2010, Groß et al. 2021) and confirmed the possibility to retro-correct with high accuracy the $\delta^{15}N$ values using the isotopic ratio measured on lipid-free aliquots.

Most lipid-normalization models for $\delta^{13}C$ could predict $\delta^{13}C_{lipid\text{-}free}$ with a satisfactory level of accuracy. The exception that stood out was the Lesage model (Eq. 5), possibly because this model is specific to cetacean skin instead of muscle or the whole organism or because it omits the C:N ratio parameter. We therefore recommend against the use of this model for estimating $\delta^{13}C_{lipid\text{-}free}$ in muscle tissue and instead suggest using the Logan or MM models, as they performed generally better in most cases.

4.3. Model specificity

Increasing model specificity from a generalized model to a species-specific model or by using coefficients optimized for the study data set reduced the MAE in all models and for both isotopes, a finding that is consistent with previous studies (Logan et al. 2008, Lesage et al. 2010, Cloyed et al. 2020). Our results, however, indicate that an intermediate scenario in which species are grouped based on their C:N ratio (cluster-based scenario) may still achieve high accuracy without the drawbacks, labor intensity, and costs of an approach whereby each species is analyzed individually, with the additional issues arising with rare species and small sample sizes. Our sensitivity analysis indicated that while some species may change clusters depending on data sets, the stability in the number of clusters generated, high probability of species being adequately classified, and minor change in model performance with a much-reduced data set suggest some robustness of this approach to data sets of varying composition and size.

Models for retro-calculating $\delta^{15}N_{bulk}$ performed as well as the $\delta^{13}C$ lipid-normalization models in 3 scenarios (i.e. global approach, cluster-based, species-specific). Worth noting is the fact that model fit was higher for the cluster-based scenario than the global model (global approach scenario) in both isotopes. These results are important, as they can help define a way forward to deal with lipid effects or lipid-extraction biases in isotopic studies depending on the specifics of each data set.

The decision tree for how to proceed depends largely on species identity. In cases where the species exists in our data set, isotopic analyses of lipid-free samples with subsequent correction of $\delta^{15}N_{lipid\text{-}free}$ values using the model and coefficient most suited to

the species under study (Fig. 3, Tables 4 & S3) would achieve the highest accuracy. An alternative approach with a slightly lower accuracy but higher labor efficiency would be to proceed with isotopic analyses on bulk samples, with a subsequent lipid-normalization of $\delta^{13}C_{bulk}$ values, again using the model (likely the Logan model) and coefficient most suited to the species under study.

In cases where the species does not exist in our data set, the investigator's decision could go 2 ways. In cases where the $C:N_{bulk}$ would not be expected to be out of range compared to values in our study, the preferred approach would be to proceed with isotopic determination from lipid-free samples, with subsequent restoration of $\delta^{15}N_{bulk}$ using the generalized equation, which achieves higher accuracy than lipid-normalization based on all samples combined but with acceptance of a potential loss of accuracy for some species over a cluster-based approach. Alternatively, the investigator could proceed with isotopic determination from bulk samples. For species with a $C:N_{bulk}$ ratio and $\delta^{13}C_{bulk}$ values within the range of the species examined in our study, investigators could attempt a correction by selecting the appropriate coefficients and cluster based on the mean $C:N_{bulk}$ ratio and $\delta^{13}C_{bulk}$ of their species. We recommend against opting for the most phylogenetically related species since there was no apparent phylogenetic kinship in the cluster composition. If the $C:N_{bulk}$ ratio value of the species ends up being out of range, the investigator should, as a last resort, use the Logan or MM models and associated coefficients for all species combined (global approach scenario) and accept some loss in precision. When available, $\delta^{13}C$ measured on bulk samples should also be reported since they can be needed in multiple situations.

This study provides a comprehensive and critical review of existing approaches to lipid effects in isotopic studies and proposes a clear way forward for obtaining reliable $\delta^{13}C$ and $\delta^{15}N$ values without incurring the costs of duplicate analyses. As such, it represents a major step toward the harmonization of data sets collected as part of long-term studies.

Acknowledgements. The authors thank the many people and organizations who have participated in bringing together this vast collection of samples, especially C. Nozères, Y. Morin, K. Gavrilchuk, D. Archambault, G. Chouinard, S. Bérubé, H. Bourdages, M. Hammill, S. Mongrain, P. Joly, S. Plourde, P. Rivard, G. Cyr, R. Dubé, B. Sainte-Marie, and the field crew of the CCGS 'Teleost', CCGS 'Leim and Lampsilis', the Québec Marine Mammal Emergency Response Network, Mingan Islands Cetacean Study, J. Gauthier (Pêcheries Charlevoix), P. Lizotte (Pêcheries Lizotte), and Ministère des Forêts, de la Faune et des Parcs du Québec. Sample preparation was conducted by Fisheries and Oceans Canada (DFO) personnel: Y. Morin, D. Gaspard, C. Potvin, K. Gavrilchuk, S. Aucoin, L. Bennour, M.-È. Chartrand-Lemieux, J. Riopel, C. Tessier-Larivière, M. Unger, and P. Gagnon. Training in mixture models was provided by G. Pigeon. We also thank R. Drimmie and M. Stas, the technical staff from the Isotope lab at the University of Waterloo, and Isotope Tracer Technologies (Ontario) for the isotopic analyses. We are grateful to 3 anonymous reviewers for thoughtful revision of the manuscript. This research project was funded under the St. Lawrence Action Plan-Vision 2000, Species at Risk program and Whales Initiatives research program of DFO, the Green Plan of Parks Canada, and the Mingan Islands Cetacean Study. Specimens and sample collection were entirely conducted under permits delivered by the DFO. Data presented in this study are archived in Government of Canada facilities and are available upon request from V.L.

LITERATURE CITED

Bourdages H, Brassard C, Desgagnés M, Galbraith P and others (2019) Preliminary results from the groundfish and shrimp multidisciplinary survey in August 2018 in the estuary and northern Gulf of St. Lawrence. Can Sci Advis Sec Res Doc 2019/037

Choy ES, Roth JD, Loseto LL (2016) Lipid removal and acidification affect nitrogen and carbon stable isotope ratios of beluga whales (*Delphinapterus leucas*) and their potential prey species in the Beaufort Sea ecosystem. Mar Biol 163:220

Clark CT, Horstmann L, Misarti N (2019) Lipid normalization and stable isotope discrimination in Pacific walrus tissues. Sci Rep 9:5843

Cloyed CS, DaCosta KP, Hodanbosi MR, Carmichael RH (2020) The effects of lipid extraction on $\delta^{13}C$ and $\delta^{15}N$ values and use of lipid-correction models across tissues, taxa and trophic groups. Methods Ecol Evol 11:751–762

DeNiro MJ, Epstein S (1977) Mechanism of carbon isotope fractionation associated with lipid synthesis. Science 197: 261–263

Fagan KA, Koops MA, Arts MT, Power M (2011) Assessing the utility of C:N ratios for predicting lipid content in fishes. Can J Fish Aquat Sci 68:374–385

Fischer-Rush J, Rochette R, Paton E, Dickey A, Hayden B (2021) An arithmetic correction for the effect of lipid on carbon stable isotope ratios in muscle and digestive glands of the American lobster (*Homarus americanus*). Rapid Commun Mass Spectrom 35:e9204

Folch J, Lees M, Sloane Stanley GH (1957) A simple method for the isolation and purification of total lipids from animal tissues. J Biol Chem 226:497–509

Fry B (2002) Stable isotopic indicators of habitat use by Mississippi River fish. J N Am Benthol Soc 21:676–685

Fry B, Baltz DM, Benfield MC, Fleeger JW, Gace A, Haas HL, Quiñones-Rivera ZJ (2003) Stable isotope indicators of movement and residency for brown shrimp (*Farfantepenaeus aztecus*) in coastal Louisiana marshscapes. Estuaries 26:82–97

Geraci JR, Lounsbury VJ (1993) Marine mammals ashore: a field guide for strandings. Texas A&M Sea Grant College Program, Galveston, TX

Groß J, Fry B, Burford MA, Bengtson Nash S (2021) Assessing the effects of lipid extraction and lipid correction on

stable isotope values ($\delta^{13}C$ and $\delta^{15}N$) of blubber and skin from southern hemisphere humpback whales. Rapid Commun Mass Spectrom 35:e9140

Grothendieck G (2022) nls2: non-linear regression with brute force. R package version 0.3-3. https://CRAN.R-project.org/package=nls2

Grün B, Leisch F (2007) Fitting finite mixtures of generalized linear regressions in R. Comput Stat Data Anal 51: 5247–5252

Grün B, Leisch F (2008) flexMix version 2: finite mixtures with concomitant variables and varying and constant parameters. J Stat Softw 28(4):1–35

Hamel S, Yoccoz NG, Gaillard JM (2017) Assessing variation in life-history tactics within a population using mixture regression models: a practical guide for evolutionary ecologists. Biol Rev Camb Philos Soc 92:754–775

Hobson KA (1999) Tracing origins and migration of wildlife using stable isotopes: a review. Oecologia 120:314–326

Hobson KA, Schell DM, Renouf D, Noseworthy E (1996) Stable carbon and nitrogen isotopic fractionation between diet and tissues of captive seals: implications for dietary reconstructions involving marine mammals. Can J Fish Aquat Sci 53:528–533

Hobson KA, Fisk A, Karnovsky N, Holst M, Gagnon JM, Fortier M (2002) A stable isotope ($\delta^{13}C$, $\delta^{15}N$) model for the North Water food web: implications for evaluating trophodynamics and the flow of energy and contaminants. Deep Sea Res II 49:5131–5150

Leisch F (2004) flexMix: a general framework for finite mixture models and latent class regression in R. J Stat Softw 11(8):1–18

Lerner JE, Hunt BPV (2022) Experimental validation confirms a carbon stable isotope lipid normalization procedure for Pacific salmon. Mar Ecol Prog Ser 698:191–197

Lesage V, Hammill MO, Kovacs KM (2001) Marine mammals and the community structure of the Estuary and Gulf of St Lawrence, Canada: evidence from stable isotope analysis. Mar Ecol Prog Ser 210:203–221

Lesage V, Morin Y, Rioux È, Pomerleau C, Ferguson SH, Pelletier É (2010) Stable isotopes and trace elements as indicators of diet and habitat use in cetaceans: predicting errors related to preservation, lipid extraction, and lipid normalization. Mar Ecol Prog Ser 419:249–265

Logan JM, Jardine TD, Miller TJ, Bunn SE, Cunjak RA, Lutcavage ME (2008) Lipid corrections in carbon and nitrogen stable isotope analyses: comparison of chemical extraction and modelling methods. J Anim Ecol 77:838–846

McConnaughey T, McRoy CP (1979) Food-web structure and the fractionation of carbon isotopes in the Bering Sea. Mar Biol 53:257–262

Perrin G, Plourde S, DiBacco C, Winkler G, Sirois P (2014) Tracing the origins of *Calanus* sp. in the Saguenay-St. Lawrence Marine Park (Québec, Canada) using $\delta^{13}C$ as a marker. Mar Ecol Prog Ser 499:89–102

Peterson BJ, Fry B (1987) Stable isotopes in ecosystem studies. Annu Rev Ecol Syst 18:293–320

Post DM (2002) Using stable isotopes to estimate trophic position: models, methods, and assumptions. Ecology 83: 703–718

Post DM, Layman CA, Arrington DA, Takimoto G, Quattrochi J, Montana CG (2007) Getting to the fat of the matter: models, methods and assumptions for dealing with lipids in stable isotope analyses. Oecologia 152:179–189

R Core Team (2022) R: a language and environment for statistical computing. R Foundation for Statistical Computing, Vienna

Rioux È, Pelletier F, St-Laurent MH (2019) Influence of lipids on stable isotope ratios in mammal hair: highlighting the importance of validation. Ecosphere 10:e02723

Skinner MM, Martin AA, Moore BC (2016) Is lipid correction necessary in the stable isotope analysis of fish tissues? Rapid Commun Mass Spectrom 30:881–889

Stephens RB, Ouimette AP, Hobbie EA, Rowe RJ (2022) Reevaluating trophic discrimination factors ($\Delta\delta^{13}C$ and $\Delta\delta^{15}N$) for diet reconstruction. Ecol Monogr 92:e1525

Vander Zanden MJ, Clayton MK, Moody EK, Solomon CT, Weidel BC (2015) Stable isotope turnover and half-life in animal tissues: a literature synthesis. PLOS ONE 10: e0116182

WoRMS Editorial Board (2022) World Register of Marine Species. https://www.marinespecies.org (accessed 2022-12-05)

Yurkowski DJ, Hussey NE, Semeniuk C, Ferguson SH, Fisk AT (2015) Effects of lipid extraction and the utility of lipid normalization models on $\delta^{13}C$ and $\delta^{15}N$ values in Arctic marine mammal tissues. Polar Biol 38:131–143

Editorial responsibility: Stephen Wing, Dunedin, New Zealand
Reviewed by: R. F. Bastos, B. Becker and 1 anonymous referee

Submitted: May 30, 2023
Accepted: April 16, 2024
Proofs received from author(s): May 29, 2024